Available online at www.sciencedirect.com

ScienceDirect

Procedia CIRP 110 (2022) 174–179

www.elsevier.com/locate/procedia

V CIRP Conference on Biomanufacturing

Aerosol Jet® Printing on stereolithography resin substrates for *in-vitro* dual bioreactor sensing

Miriam Seiti[a,b], Paola Serena Ginestra[b], Akash Verma[a], Elisabetta Ceretti[b], Eleonora Ferraris[a]*

[a]*Manufacturing Processes and Systems (MaPS), Mechanical Engineering, KU Leuven, Sint Katelijne Waver, 2860, Belgium*

[b]*Department of Mechanical and Industrial Engineering, University of Brescia, Brescia, 25123, Italy*

* Corresponding author. *E-mail address:* eleonora.ferraris@kuleuven.be

Abstract

Aerosol Jet® Printing (AJ®P) is a relatively novel additive manufacturing technique, of the type direct writing, principally applied for printed electronics. Particularly, AJ®P has the ability to print various functional inks (conductive, dielectrics, biological solutions) at micro-scale resolution and on *free-from* substrates. This work investigates AJ®P to fabricate conductive patterns on stereolithography (SLA) samples towards the development of an innovative bioelectrical device for *in-vitro* dual bioreactor sensing. Silver nanoparticle (AgNPs) and poly(3,4-ethylenedioxythiophene) polystyrene sulfonate (PEDOT:PSS) inks were both tested. Preliminary results show a low metal-polymer AgNPs–SLA interaction, revealing the presence of pores and cracks along with the printed pattern after thermal sintering, with no electrical resistance (R) detected. In contrast, the PEDOT:PSS ink reveals a good covering of the SLA samples, with R decreasing with the number of printed layers (from ~700 kΩ to ~60 Ω for 15 and 40 layers, respectively, on lines 1 cm long). However, using the PEDOT:PSS ink, the total printing time was ~45 minutes, hence not ideal for an industry-oriented vision. Therefore, a study on the optimization of the AgNPs–SLA sample interaction was carried out. SLA samples were coated with Parylene-C (ParC), and further treated with a low pressure plasma. The final results show excellent conductivity (R~2.40 Ω), with a printing time of ~5.5 minutes (7 layers), demonstrating the possibility to obtain a functional circuit. Eventually, the circuit was encapsulated with polydimethylsiloxane (PDMS) in order to avoid a release of Ag^+ ions, potentially toxic in the medium culture.

Keywords: Aerosol Jet® Printing; Stereolithography; bioelectronics, tissue engineering, ink-substrate interaction;

1. Introduction

Tissue engineering (TE) is an innovative technological area that has emerged in the last decades and is rapidly evolving, gaining importance especially in biomedical engineering and clinical research. Biologically inspired devices have been designed worldwide to mimic physiological tissues and evaluate cell response to mechanical stress, local therapies, electrical, and chemical stimuli. The fundamental molecular phenomena and cell interactions have been subject of study broadly, as a result of scaffold production and structuring. An important part of the advances in biomedical engineering has been played by the emerging of improved technologies for cell monitoring and sensing, also in a three-dimensional (3D) domain especially for electroactive cells, such as neuronal lineages [1]. Complex biochemical and biological phenomena can indeed be monitored and controlled by novel measurement technologies that allow the quantification of several parameters (e.g. cellular impedance, viability, analytes), which are crucial to fully understand the cell behavior. This multidisciplinary TE approach is also leading to the development of bioreactors chambers in which cell cultures can be conducted in a dynamic way to promote the 3D colonization of the substrates tailored for a specific cell phenotype. Both on the academic and commercial point of view, the clinical pressure for replacement and regeneration of damaged tissues has to be addressed with the proper integration of biology, biomechanics, and bioelectronics. In this context, this paper aims to illustrate a

2212-8271
10.1016/j.procir.2022.06.032

possibility of sensing a bioreactor with tailored conductive patches, additively manufactured by 3D stereolithography (SLA) and functionalized with an Aerosol Jet® Printing (AJ®P) technique. The resulting bioelectrical patches will be further used in an *in-vitro* sensing chamber for cell culturing and monitoring over time. Particularly, AJ®P is a relatively novel Direct Writing (DW) technique, principally applied for two-dimensional (2D) and recently for 3D applications in printing of electronics (PE), bioelectronics, and biological interfaces. AJ®P enables the printing of an aerosolized and focused jet at micro-scale resolutions down to 15 µm (X-Y plane) and ~100 nm (thickness). In detail, this technique is able to deposit functional inks of different nature (e.g. conductive, dielectrics, or biological solutions[2–4]), with a wide range of viscosity (1-1000 cP), on free-form (such as 2D, 3D, rigid or flexible) substrates. The AJ®P is here investigated for the fabrication of conductive patterns, in the form of lines and arcs, on SLA substrates. Two PE inks are selected, tested and compared each other. They are: i) an own-developed poly(3,4-ethylenedioxythiophene) polystyrene sulfonate (PEDOT:PSS-based) ink, and ii) a commercial silver nanoparticle (AgNPs-based) ink. Optimization studies of the ink-substrate interaction, geometrical patterns, and printing parameters are performed to improve ink adhesion, printability, and electrical performances. Eventually, the most suitable ink-substrate combination is further investigated towards an industry-oriented vision.

2. Materials and Methods

2.1 Inks and substrates

An own-developed PEDOT:PSS-based ink and a commercial AgNPs-based ink are selected as AJ®P materials. PEDOT:PSS and AgNPs dispersions are considered the most available, used, and performant inks in the PE industry. PEDOT:PSS inks are preferred in terms of cost and biocompatibility, while AgNPs inks for conductivity and printing efficiency. Here, both inks are investigated in order to find the best candidate for an industry-oriented vision. Particularly, **Table 1** reports a comparison of the main properties and composition of the inks. The PEDOT:PSS (1.3wt%) ink is an aqueous-based dispersion, enhanced with the addition of polyethylene glycol (PEG) and carboxymethyl cellulose (CMC) for a better conductivity and chemical stability. The ink is retained biocompatible, with preliminary good results on human induced pluripotent stem cells (iPSCs) derived neurons, by means of a cytotoxic rATP direct assay up to 72 hours [5]. Alternatively, the AgNPs-based ink is a water-based commercial solution (Novacentrix, Metalon® JS-ADEV N250, USA), with a 40-60 wt% Ag loading content (average particle size of 50 nm), 3-10 wt% diethylene glycol (DEG), and 2-10 wt% isopropanol (IPA), as from data-sheet. A polyurethane (PU) component was also added with a proportion of 3:100 to Ag to improve adhesion to various substrates. Differently from the previous ink, AgNPs-based inks are known to potentially release Ag^+ ions in the medium culture, inducing a high *in-vitro* cytotoxicity, such as with neuronal lineages [3]. On the other side, the AgNPs-based ink owns an electrical resistivity (ρ_{Ag} = 3x10^{-5} Ω·cm) 2 orders of magnitude lower than PEDOT:PSS one (ρ_P = 1.66x10^{-3} Ω·cm).

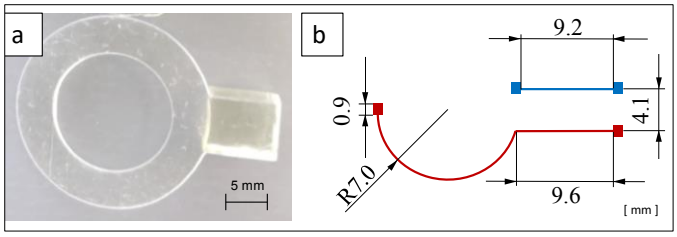

Figure 1. Representative image of (a) the SLA printed substrate, and (b) geometrical dimensions [mm] of the conductive patterns (line in blue, arc in red) and pads (square) to be printed (designed by IVTech Srl, IT).

Table 1. Main properties of PEDOT:PSS- and AgNPs-based inks.

Inks properties		
Ink	PEDOT:PSS-based (1.3wt%)	AgNPs-based (40-60 wt%)
Main solvent	Water	
Viscosity, η [mPas]	10-20	≤ 10
Surface tension, σ[mN/m]	75	70
Resistivity, ρ [Ω·cm]	1.66x10^{-3}	3.0x10^{-5}

The substrates were fabricated by a stereolithography (SLA) AM technique (Prusa© SL1 3D printer, PRAG), using a Clear and Tough Resin (3Dresyns©, ES). The design was chosen according to the bioreactor chamber geometry, and it consists of a disk shape with an external diameter $Ø_{ext}$ = 21 mm, an internal one of $Ø_{int}$ = 13 mm, and a thickness of t = 0.25 mm (see **Figure 1a**). Post-printing processes were performed by means of a Prusa Curing and Washing Machine (CW1, Prusa©, PRAG). Glass slides (Superfrost VWR, BE) and Polyethylene terephthalate (PET) (Melinex® ST506, DuPONT Teijin Films™, USA) thin films, were used as reference substrates (positive control), respectively for PEDOT:PSS-based and AgNPs-based inks.

2.2 Print strategy and investigation

An AJ®P Optomec© 300 series system (USA) was used to print the electrical circuit on the SLA substrates. The designed geometry of the circuit is visible in **Figure 1b**. The pre-requisite value of electrical resistance (R, [Ω]) for the final application is $R_{target} \leq$ 50 Ω, with no presence of cracks along the circuital patterns, that is: a line and an arc connected with a line (here named as arc), both with contact pads at their edges. The circuit should have a line width and a thickness around 100 µm and 10 µm, respectively. Moreover, the circuit should be printed on the SLA substrate in such a way that the contact positions are centrally aligned with the final device. For these reasons, a .dxf file of the circuit was designed in AutoCAD to meet the requirements, and subsequently converted in a .prg file (using VMTools), ready for the printing process. Prior printing, substrates were cleaned with distilled water (DI) (Sigma Aldrich, BE) and inks were sonicated in an ultrasonic bath at T = 25°C (EMMI - 20 HC, Emag), for 10 mins each. Additionally, SLA substrates were manually polished with an emery paper (P2400 grit, grain size 8.4 µm) for 2 minutes to obtain a flat, smooth, and grease-free surface.

Ink and Printing parameters													
Printer and environmental conditions	AJ®P Optomec AJ300s (USA), (23°C, 50% rh)												
Ink	PEDOT:PSS-based ink, 850 µL							AgNPs-based ink, 1.5 mL					
Substrates (reference and target)	Glass Slides			SLA substrate				PET thin film			SLA substrate		
Print strategy - Offset, *z* [mm]	LBL approach – 3												
Nozzle, *Ø* [µm]	300												
Sheath gas flow, *SGF* [sccm]	40			50				75					
Carrier gas flow, *CGF* [sccm]	40							20					
Platen temperature, *T* [°C]	40			80				25					
Printing speed, *s* [mm/sec]	7			10				6					
Line width, *l* [µm]	100			100	500	700	800	100			150		800
Number of layers, *n* [#]	25	50	75	40				2	5	10	7		
Post-processing	Thermal annealing (150 °C, 1h)							Thermal sintering (PET 200°C, 1h – SLA 150 °C, 2h)					
Output	Electrical Resistance, *R* [Ω]												

Table 2. Details of the experimental campaigns on the AJ®P process applied on AgNPs-based and PEDOT:PSS inks on different substrates.

Details on the experimental campaigns are reported in **Table 2.** Each ink was atomized in a glass vial at 25°C in an AJ®P ultrasonic bath at 49.5 V. Every three hours of continuous printing, the vial was refilled (850 µL and 1.5 mL, respectively for PEDOT:PSS-based and AgNPs-based ink) and a buffer time of ~5 min was used afterwards to reduce system drifting and to reach a stable jet flow. Prior printing, substrates were positioned on the platform for ~10 min to reach a thermal equilibrium with the platen temperature.

Process parameters were then investigated with a layer-by-layer (LBL) approach in order to study print feasibility. Five main printing parameters were considered: the nozzle diameter (*Ø,*[µm]), the focusing ratio (R_f,[#]), the platen temperature, (*T,* [°C]), the printing speed (*s,* [mm/s]), and the number of printed layers (*n,* [#]). In particular, the R_f is defined as the ratio between the sheath gas flow (*SGF*, [sccm]), and the carrier gas flow (*CGF*, [sccm]) (usually > 1). The SGF dictates the jet focusing at the level of the print head, thus at the exit of the nozzle, while the CFG indicates the amount of aerosolized ink transported from the atomizing vial to the print head. In both cases, nitrogen (N_2) was used as inert gas. Printing parameters were selected based on previous expertise on same reference substrates [6], and later fined-tune by a trial & error approach on the SLA substrate. Subsequently, two investigations were performed on both inks over the influence of the number of printed layers, *n*, and the line width of the circuit, *l*, with *R* as output. In details, the first study deals with the printing of the circuit on the reference substrates (glass and PET), at the desired l = 100 µm and by changing *n*. Based on the results obtained in terms of *R*, a second study was then carried out, by fixing *n* and modifying *l* in the range of 100-800 µm. A trade-off between printing time, shape accuracy, and inks resistivity, was considered for the choice of *n*. The total *n* indeed dictates the printing time, and it was fixed differently for each ink based on their conductivity. Moreover, as each printed layer is deposited on the top of each other (wet-on-wet), a decrease in shape fidelity becomes evident by increasing *n,* due to ink spreading which causes waved edges. After fixing *n*, *l* was then increased in order reach R_{target}. A minimum of three repetitions were performed for each combination. After printing, the samples were cured in a thermal oven (Heraeus, DE).

2.3 Samples characterization

Ink-substrate interactions were analyzed for each combination in order to verify if the resulting values on reference and final substrates were similar to justify the use of same printing parameters. Contact angle (CA, [°]) (Contact Angle Goniometer, Ossila, UK) analyses were executed with a 25µl glass syringe at two different time points t_1 = 10 s and t_2 = 120 s. Surface energies, γ [mN/m], were estimated with test inks of known γ (Series A, Tigres, GmbH). For both evaluations, 3 representative samples were tested 3 times each, for a total of 9 measurements. Electrical resistances *R* of the printed circuits were recorded three times per sample, by means of a two-point probe method (Digital Multimeter, DM3068, Rigol, USA), when possible. Visual inspection was performed with an optical microscope (Hirox KH – 8700, JP) and a Scanning Electron Microscope (SEM, VEGA3 Tescan, PRAG). In the case of the AgNPs-based ink, a layer of Parylene-C (ParC), ca. 3 µm thick, was chemically vapour deposited (CVD) onto SLA substrates. Subsequently, a N_2 surface plasma (Tergeo Plasma Cleaner, pPIE Scientific LLC, USA) treatment (20 secs, 50 W) was performed to increase the wettability of the ParC-SLA substrate. In *Section 3*, the subscripts $_P$ and $_{Ag}$ are used to refer the corresponding ink.

3. Results and discussion

3.1. AJ®P of PEDOT:PSS-based ink

A first set of 8 samples were printed with the PEDOT:PSS-based ink on glass substrates, with a line width l = 100 µm, and printing parameters as $Ø_P$ = 300 µm, $R_{f,P}$ = 1, s_P = 7 mm/s, and n_P = 25, 50, and 75. The ink was then annealed at 150°C for 1 hour. As shown in **Figure 2a**, an increase in *n* is inversely proportional to *R*, up to a minimum of $R_{P,\,Glass,\,Line}$ = 1.7 kΩ and $R_{P,\,Glass,\,Arc}$ =5.7 kΩ at *n* =75. Despite a good ink printability,

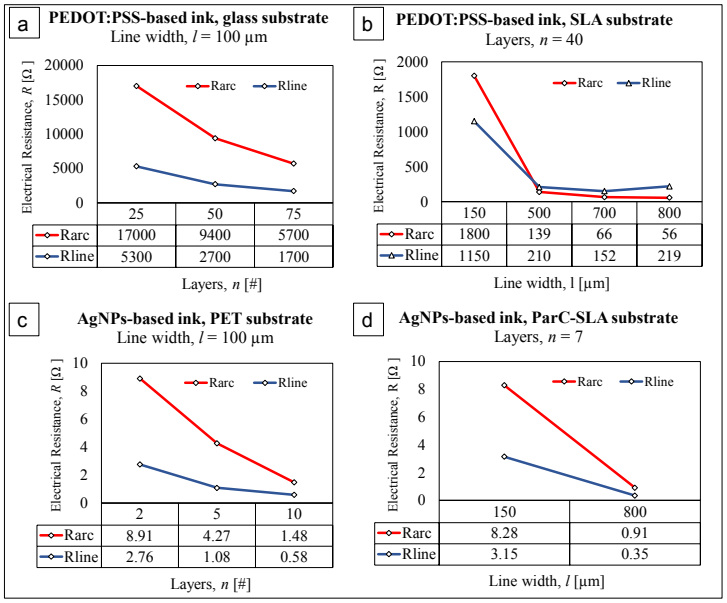

Figure 2. Electrical resistance values on (a) AJ® printed circuit with PEDOT:PSS-based ink on glass substrates at a fixed line width l = 100 µm, and (b) on SLA substrates at a fixed number of layers n = 40; (c) AJ® printed circuit with AgNPs-based ink on PET substrates at a fixed line width l = 100 µm, and (d) on ParC-SLA substrates at a fixed number of layers n = 7.

Table 3. *Contact angle and surface energy measurements.* CA are performed on SLA bare and polished substrates both for AgNPs-based and PEDOT:PSS-based inks. Additional CA are performed for AgNPs-based ink on ParC-SLA, plasma ParC-SLA, and PET substrates, and for PEDOT:PSS-based ink on glass substrate. Surface energies are reported for every substrate used.

Contact Angle Measurements, CA [°]								
	PEDOT:PSS-based ink			**AgNPs-based ink**				
Time	SLA bare substrate	SLA polished substrate	Glass substrate	SLA bare substrate	SLA polished substrate	ParC-SLA substrate	Plasma ParC-SLA substrate	PET substrate
t_1= 10 s	63.84±3.6°	64.73±6.5°	53.21±3.1°	44.39±5.2°	28.66±4.9°	50.72±4.9°	7.82±0.5°	43.07±2.4°
t_2 = 120 s	58.34±2.2°	49.23±3.9°	45.82±4.2°	34.36±4.6°	21.83±3.8°	37.35±7.5°	≤ 3°	31.32±7.1°

Surface Energy Measurements, γ [mN/m]					
SLA bare substrate	SLA polished substrate	ParC-SLA substrate	Plasma ParC-SLA	PET substrate	Glass substrate
42-44	38-40	32-34	42-40	38-40	38-40

the R detected is still too distant from $R_{target} \leq 50$ Ω due to the geometrical dimensions of the circuit. Additionally, n = 75 requires a printing time of ca. 2 hours/sample, which is considered too high for an industry-oriented setup. To further reduce R, a second study was performed by gradually increased l from 100 µm till 800 µm. This experiment was directly performed on polished SLA substrates since their wettability measurements reveal a $CA_{polished\ SLA-P}$ = 49.23° ± 3.9°, very close to the $CA_{glass-P}$ = 45.82° ± 4.2° (t_2 = 120 s). Specifically, polished SLA substrates were preferred to bare SLA substrates for their smoothness, which results in a CA reduction of ca. 15.6% (t_2 = 120 s). Similarly, γ gets reduced from $\gamma_{bare\ SLA}$ = 42-44 mN/m to $\gamma_{polished\ SLA} = \gamma_{glass}$ = 38-40 mN/m (**Table 3**). Printing parameters were slightly changed as: s_P from 7 to 10 mm/s (to ensure printing stability), and $R_{f,P}$ from 1 to 1.25 (for a wider print deposition). Moreover, n was selected equal to n_P = 40. **Figure 2b** depicts a lower bound in R starting from 500 µm, equal to $R_{P,\ SLA,\ Line}$ = ca. 60 Ω and $R_{P,\ SLA,\ Arc}$ in the range [150-220] Ω (SLA substrate). A printing time of ~45 mins/sample was necessary to obtain the final printed circuit. **Figures 3a** and **3b** display the AJ® printed circuit on SLA substrates at l_1 = 100 µm with n_1 = 25, and at l_2 = 800 µm with n_2 = 40. Despite electrical results are retained satisfactory on R_{line}, R_{arc} and the printing time are still not ideal in terms of conductivity and printing efficiency. A parallel study on the use of AgNPs-based ink is then pursued in *Section 3.2*.

3.2. AJ®P of AgNPs-based ink

In order to study a more efficient print, an AgNPs-based ink was investigated and compared to the PEDOT:PSS-based ink in terms of printing time and electrical performances.

Printing conditions were previously tested on a PET thin film as reference substrate (**Figure 2c**). A first set of samples were printed at l = 100 µm, with $Ø_{Ag}$ = 300 µm, $R_{f,\ Ag}$ = 3.75, s_{Ag} = 6 mm/s, and n_{Ag} = 2, 5, and 10. The ink was then annealed at 200°C for 1 hour. Electrical resistances were detected equal to $R_{Ag,\ PET,\ Arc}$ = 0.58 Ω and $R_{AgNPs,\ PET,\ Line}$ = 1.48 Ω on circuits printed in ~7 minutes and n = 10, demonstrating ink-printing process functionality to achieve (**Figure 4a**). SEM images, reported in **Figures 4b** and **4c**, verify excellent ink printability and a smooth, conductive surface of the printed line, without

pores and/or cracks. The same printing conditions were then applied on the SLA substrates. As a metal-based ink, the AgNPs-based ink requires higher sintering temperatures than a polymer ink. Specifically, the temperature should be in the range of [120-250]°C, for minimum 1 hour, in order to obtain a conductive pattern. Due to the final application which requires substrate transparency, an analysis at different sintering temperatures was conducted on the substrate. As shown in **Figures 4d** and **4f**, a gradual increase in yellowing of the SLA substrate is visible starting from 160°C, along with the presence of multiple fractures through the surface, due to resin degradation. Since a lower sintering temperature was then required to maintain transparency, it was chosen to sinter the green parts at 150°C for a longer time, that is 2 hours. Preliminary observations on the printing process indicates a low metal-polymer AgNPs–SLA interaction, revealing the presence of cracks along the sintered printed patterns, with no *R* detected (**Figures 4e** and **4f**). This can be correlated to two crack stress phenomena (initiation and propagation) during the sintering process. First, the printed wet ink faces a capillary-pressure driven crack formation from room to sintering temperature [7], which results in the formation of micro-cracks due to a fast (co)-solvents evaporation rate. Secondly, the phenomenon is emphasized by a shrinkage-induced crack formation during the sintering process. This is mostly caused by expansions of ink and substrate at different rates, due to a difference in the coefficients of thermal expansion. As for the PEDOT:PSS ink, a fine grain polishing was performed for 2 minutes on each SLA substrate in order to increase the ink-substrate adhesion. However, no satisfactory improvements were observed, despite an increase in the surface smoothing and an improvement in wettability from $CA_{bare\ SLA\text{-}Ag}$ =34.36° ± 4.6° to $CA_{polished\ SLA\text{-}Ag}$ =21.83° ± 3.8°, which is 30.3% lower than $CA_{PET\text{-}Ag}$ =31.32° ± 7.1°, and also demonstrated by an equal $\gamma_{polished\ SLA} = \gamma_{PET}$ = 38-40 mN/m (**Table 2**). As reported in **Figure 4g**, pores of maximum size ca. 1 µm, are still present all over the surface, impeding the passage of electrical current. Thus, a coating of the SLA samples was necessary with a material ideal for printing. The insulating crystalline polymer ParC was selected due to its biocompatibility, optical transparency, high thermal stability, and proven printability (if activated with a plasma treatment [6]). As shown in **Table 2**, $CA_{plasma,\ ParC\text{-}SLA\text{-}Ag} \leq 3°$ is 91.9% lower than $CA_{ParC\text{-}SLA\text{-}Ag}$ = 37.35° ± 7.5°, with a changed in γ from $\gamma_{ParC\text{-}SLA}$ = 32-34 mN/m to $\gamma_{plasma,ParC\text{-}SLA}$ = 40-42 mM/m. Same printing conditions were then applied on plasma ParC+SLA substrates. In this case, successful conductive circuits were printed at l = 150 µm in ca. 5.5 mins/sample, with final $R_{Ag,\ ParC+SLA,\ Arc}$ = 8.28 ± 3.08 Ω and $R_{Ag,\ ParC+SLA,\ Line}$ = 3.15±1.24 Ω, on a total of 11 samples (**Figure 3c**). In order to further demonstrate the ability of AgNPs-ParC+SLA to obtain highly conductive tracks, l was increased up to 800 µm, showing values of $R_{Ag,\ ParC+SLA,\ Arc}$ = 0.91 Ω and $R_{Ag,\ ParC+SLA,\ Line}$ = 0.35 Ω (**Figures 2d** and **3d**).

3.3 Circuit optimization

The AgNPs-based ink was eventually chosen to print circuits *in series* on plasma activated ParC-substrates. In the vision of a product industrialization, the printing tolerance and time per

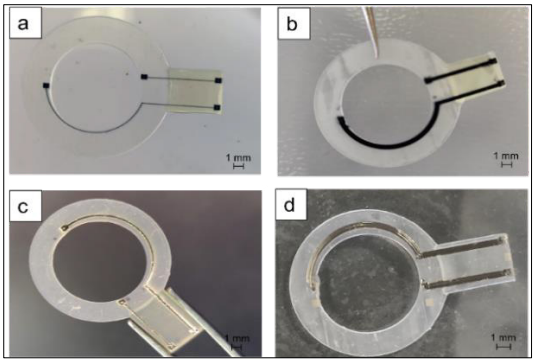

Figure 3. AJ® printed circuit on SLA substrates with PEDOT:PSS-based ink at a (a) line width l_1 = 150 µm, number of layers n_1 = 40, $R_{P,\ Arc,\ 1}$ = 1800 Ω, and (b) at l_2 = 800 µm, n_2 = 40, $R_{P,\ Arc,\ 2}$ = 56 Ω, with a printing time of ~45 mins/sample; same circuit printed on ParC-SLA substrates with AgNPs-based ink, at a (c) l_3 = 150 µm, n_3 = 7, $R_{Ag,\ Arc,\ 1}$ = 8.28 Ω and (d) a l_4 = 800 µm, $R_{Ag,\ Arc,\ 2}$ = 0.91 Ω at n_4 = 7, with a printing time of ~7 mins/sample.

batch were improved by the fabrication of a supporting mask. As shown in **Figures 5a** and **5b**, a SLA printed mask was used for the consecutive printing of 8 circuits. This mask also facilitates the alignment and printing of the circuit onto the substrate, favouring production repeatability and control of tolerances. Moreover, due to the proven *in-vitro* cytotoxicity of AgNPs, the circuit was encapsulated in order to impede the release of Ag^+ ions in the medium culture. Polydimethylsiloxane (PDMS) was chosen as encapsulating material due to its wide proven biocompatibility when in contact with cellular systems, optical transparency, impermeability, and hysteresis-free nature. Moreover, a polymer-polymer interaction between PDMS and ParC-SLA substrate is preferred. A solution of Sylgard 184 PDMS (Dow Corning, USA) was manually poured on the samples by means of a spatula, followed by a curing process of 5 hours at 60°C in an oven and subsequently 48 hours at room temperature. The ratio for transparent PDMS solution used was 10:1 w/w (Part A&B). Electrical resistances were then verified ($R_{target} \leq 50$ Ω) on a total of 9 samples on the contact pads, having $R_{Ag,\ Final\ sample,\ Arc}$ = 11.84 ± 0.01 Ω and $R_{Ag,\ Final\ sample,\ Line}$ = 4.95 ± 0.08 Ω. **Figure 5c** gives a representative overview of the final samples.

4. Conclusion and future perspectives

The development of sensing bioreactors chambers for dynamic 3D cell culturing and activity monitoring is a current trending topic. In this manuscript, an investigation on the use of the AJ®P technology on SLA printed samples is performed for the final fabrication of conductive patches for *in-vitro* dual bioreactors sensing. The target circuit comprises an arc and a line, both with contact pads at their edges, and with a final $R_{target} \leq 50$ Ω. Moreover, the circuit should be centrally aligned onto the SLA sample. Thus, two conductive inks, an own-developed PEDOT:PSS-based and a commercial AgNPs-based ink, are tested and compared in the vision of a potential industrialization, particularly in terms of substrate adhesion, printability, and conductivity performances. Despite a good wettability on polished SLA samples, preliminary results on the AgNPs-based ink show a low metal-polymer AgNPs–SLA interaction, with presence of cracks and pores along the printed patterns after sintering. Consequently, no *R* was detected. This is mostly caused by a crack stress phenomenon, which hinders the percolation path of sintered AgNPs. In contrast, the

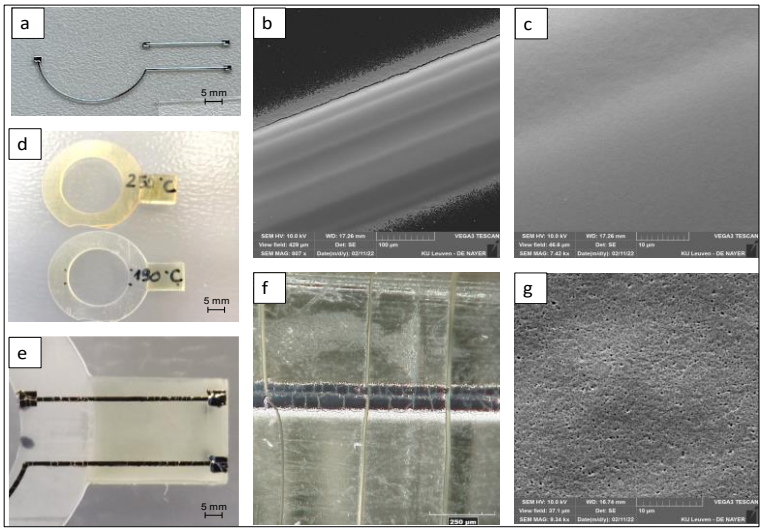

Figure 4. Representative pictures on the use of the AgNPs-based ink: (a) an AJ® printed circuit on a PET reference substrate, along with SEM images of (b) the printed line and (c) the smooth surface, demonstrating an excellent ink deposition and sintering; (d) gradual yellowing of the SLA substrate due to an increase in the sintering temperature, at 190 °C and 250 °C, respectively; (e) detail on a AJ® printed circuit on a polished SLA substrate, sintered at 150 °C for 2 hours, with evidence of cracks, due to a not ideal metal-polymer interface; (f) zoom of an AJ® printed line on SLA substrate, with ink and substrate cracks, sintered at 180 °C for 1 hour; g) SEM image of the printed ink surface on a SLA substrate, with clearly visible pores of maximum ca. 1 µm, resulting in a non-conductive pattern.

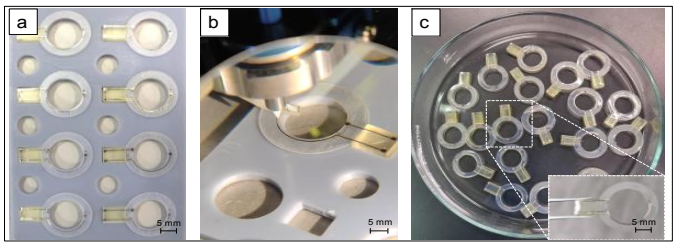

Figure 5. Representative images of: (a) the supporting SLA printed mask, capable of hosting up to 8 circuits; (b) the AJ®P process of the AgNPs-based ink on the plasma-activated ParC-SLA substrate, with the use of the mask; (c) the final PDMS-coated AgNPs+ParC-SLA samples.

PEDOT:PSS-based ink demonstrated a good wettability and deposition, with a final R_{arc}~60 Ω. Regardless delivering satisfactory results, PEDOT:PSS-based ink is not ideal in terms of printing time (ca. 45 mins/sample) and limited conductivity. An optimization study on the AgNPs–SLA interaction is then performed, with a plasma-activated ParC coating. Same printing conditions used for uncoated SLA substrates, were here applied and conductive patches with l = 150 µm and printing time of ca. 5.5 mins/sample were fabricated with R_{Arc} ~ 8.3 Ω, and R_{Line} ~ 3.2 Ω. AgNPs-based ink is thus a better candidate than PEDOT:PSS-based ink, with an average reduction in R equal to $\%R_{Arc}$ = 95.5% and $\%R_{Line}$ = 94.76%. Due to a proven AgNPs cytotoxicity (if exposed to the medium culture), a PDMS encapsulation was carried out, keeping R still lower than $R_{target} \leq 50$ Ω, with R_{Arc} ~ 11.8 Ω and R_{Line} ~ 5.0 Ω.

Future works will be towards product quality improvement, with focus on resin selection and coating technique. Particularly, a different resin with higher thermal resistance will be tested to reduce deformations and yellowing, and to allow a faster ink sintering time. Moreover, ParC will be investigated as an alternative coating material to PDMS via CVD, in order to automatize the process and reduce thickness variability. A deeper understanding of the metal-polymer interaction, in terms of surface porosity, roughness, and permeability will be also carried out. Afterwards, biocompatibility and functional assays (in terms of patches sensing capabilities) will be performed in a dynamic cell-culturing. This approach, combined with engineered scaffolds, can boost the production of cell-culture systems which, can mimic the physiological environment and optimize the *in-vitro* evaluation of cells therapies and treatments.

Acknowledgements

The authors kindly acknowledge IVTech Srl (IT) for funding this work within the LiveSens project (Grant N3 ARTES 4.0 – 2020), Leonardo Riva for SLA samples fabrication, Stefania Scala for the supporting mask design, and Olivier Degryse for SEM images. We extend our gratitude to DuPont Teijin for providing PET foils, Mr. Dave Pope (Novacentrix Inc., USA) for ink details, and Research Foundation Flanders (FWO) for the doctoral fellowship granted to Miriam Seiti, 1SB1120N.

References

[1] Seiti M, Ceretti E, Ferraris E, Ranga A. Emerging Three Dimensional Integrated Systems for Biomimetic Neural In Vitro Cultures. Adv Mater Interfaces 2022;2101297.

[2] Gibney R, Patterson J, Ferraris E. High-Resolution Bioprinting of Recombinant Human Collagen Type III. Polym 2021, Vol 13, Page 2973 2021;13(17):2973.

[3] Seiti M, Ginestra P, Ferraro RM, Ceretti E, Ferraris E. Nebulized jet-based printing of bio-electrical scaffolds for neural tissue engineering: a feasibility study. Biofabrication 2020;12(2):025024.

[4] Machiels J, Verma A, Appeltans R, Buntinx M, Ferraris E, Deferme W. Printed Electronics (PE) As An enabling Technology To Realize Flexible Mass Customized Smart Applications. Procedia CIRP 2021;96:115–20.

[5] Seiti M, Ferraro RM, Ginestra PS, Ceretti E, Eleonora F, Development of a bioelectrical ink for Aerosol Jet® Printing of 3D microstructures, Biofabrication 2021, Wollongong.

[6] Seiti M, Ginestra PS, Ferraro RM, Giliani S, Vetrano RM, Ceretti E, Ferraris E, Aerosol Jet® Printing of Poly(3,4-Ethylenedioxythiophene): Poly(Styrenesulfonate) onto Micropatterned Substrates for Neural Cells In Vitro Stimulation. Int J Bioprinting 2022; 8(1):504.

[7] Dalal N, Gu Y, Hines DR, Dasgupta A, Das S. Cracks in the 3D-printed conductive traces of silver nanoparticle ink. J Micromechanics Microengineering 2019;29(9):97001